Evaluating Cellular Mechanisms of Bipolar Disorder Using 3-D Stem Cell Models of the Human Brain

By:

Henry Tran

Mentors:

Sue O'Shea: Ph.D., Crosby-Kahn Collegiate Professor of Cell and Developmental Biology, Professor of Psychiatry, Michigan Medicine

Sara Aton: Ph.D., Associate Professor of Molecular, Cellular, and Developmental Biology, University of Michigan

Durga Attili: M.S., Research Lab Specialist Senior, Cell and Developmental Biology, Michigan Medicine

Readers:

Sue O'Shea: Ph.D., Crosby-Kahn Collegiate Professor of Cell and Developmental Biology, Professor of Psychiatry, Michigan Medicine

Sara Aton: Ph.D., Associate Professor of Molecular, Cellular, and Developmental Biology, University of Michigan

Haoxing Xu: Ph.D., Professor of Molecular, Cellular, and Developmental Biology, University of Michigan

March 31st, 2021

Submitted for partial fulfillment of the Bachelor of Science degree in Molecular, Cellular, and Developmental Biology with Honors

Abstract:

Bipolar Disorder (BD) is a chronic psychiatric illness that has no definitive cause nor cure. Symptoms of BD include elevated mood swings, alternating between anger and depression with anxiety. Heritability of BD is high and specific genetic markers of BD overlap with other neuropsychiatric conditions such as schizophrenia and major depression (Gordovez, F., & McMahon, F. J., 2020). Although researchers have previously used mice or postmortem human brain tissue to investigate the cause of BD, these models fail to take into account the effects of changes in brain structure due to medication or life stressors as well as changes at death. To address cellular changes, BD can be studied using human induced pluripotent stem cells or hiPSCs. HiPSCs are pluripotent, can form all cells of the body like human embryonic stem cells (hESCs), and provide a 2-D in vitro model for BD following differentiation of hiPSCs into neurons. Recent advances have considerably improved cultures to derive 3-D brain organoids. Brain organoids have the remarkable capability to self-organize without added signals to differentiate specific brain regions, creating a 3-D model of the developing human brain. In this manuscript we obtain adult skin fibroblasts from bipolar patients and cultured them into hiPSCs. Next, we differentiated them into brain organoids and observed morphological differences between control, bipolar cells containing a SNP associated with BD, and hiPSCs that underwent gene editing to correct the SNP (CRISPR corrected brain organoids). We then looked for any transcriptional abnormalities in expression of neural markers and BD susceptibility genes such as *CACNA1C*. Using immunohistochemistry, organoid sections were also stained for neuronal markers, to identify differences in protein expression between bipolar, control, and CRISPR corrected lines on days 30, 60, and 90 of in vitro development. We found that in bipolar cell

lines, *VGLUT-1* expression levels were significantly lower compared to control and CRISPR corrected lines at day 60. *PAX6* transcripts were elevated in BD CRISPR corrected day 30 relative to BD day 30 samples which presumably produced expression of downstream targets marking glutamatergic and GABAergic neurons at day 60 as well. While these results provide useful information about the cellular mechanisms of BD, more remains to be done to discover the cause and possible treatments of BD.

Introduction:

Bipolar Disorder (BD) is a chronic psychiatric illness that displays oscillations in mood from manic to depressive episodes. It has been estimated that approximately 45 million people worldwide suffer from BD (GBD 2017 Disease and Injury Incidence and Prevalence Collaborators, 2018). In addition, BD has been associated with other comorbidities such as cardiac abnormalities and diabetes, increasing the morbidity of this condition (Kim et. al, 2017). BD proves to be challenging as people may fail to distinguish manic or depressive symptoms as illness-related, leading to delayed diagnosis (Baldessarini RJ et. al, 2007). There is a small yet consistent genetic contribution to BD but despite this, little is known regarding the molecular pathology of BD (Mendlewicz, J., Rainer, J., 1977).

Animal models such as mice are ideal for studying the basis of diseases such as Alzheimer's, but not BD. This is because symptoms such as depression and mania used to diagnose BD in humans cannot necessarily be recapitulated and identified in murine models. This is a barrier to developing human-oriented therapeutic drugs with high efficacy. Although psychostimulants such as cocaine have been used to induce mania-like behavior in mice, experts have still been unable to create murine models that show spontaneous alternating episodes of manic and depressive-like behaviors (Nestler, E., Hyman, S., 2010).

Noninvasive imaging and postmortem human brain studies have revealed neuroanatomical changes in the bipolar brain but these changes are not universal. Noninvasive human brain imaging does not provide an accurate depiction of molecular/cellular pathology to identify BD mechanisms and postmortem human brain tissue fails to highlight disease progression and treatment effects in BD patients (Wen, Z., et. al, 2016). In addition, since

postmortem human brain tissue is typically not amenable to tissue culture, the ability to derive stem cells from patients with BD provides an in vitro method to model the cellular mechanisms underlying it (Takahashi, K., et. al, 2007).

Human induced pluripotent stem cells (hiPSCs) are derived by reprogramming adult skin fibroblasts or other somatic cells via overexpression of the four "Yamanaka" factors (Oct3/4, Sox2, Klf4, and c-Myc) (Takahashi, K., et. al, 2007). High expression of these factors activate Nanog, a pluripotency gene that causes other genes involved in early human development to be activated, allowing researchers to model embryonic development in hiPSCs (Nakagawa, M., 2008). HiPSCs have the ability to differentiate into all cell types in the body including neurons. These hiPSCs are similar to human embryonic stem cells (hESCs) in terms of morphology, gene expression, and proliferation, making them a great alternative to hESCs to mitigate any ethical concerns. The fact that adult somatic fibroblasts can be turned back into hiPSCs allows researchers to derive patient specific disease models. Furthermore, hiPSCs make genetic studies of neuropsychiatric disorders more feasible, since the unique genome of the donor is retained and one can study the progression of BD for example throughout differentiation (Christian K.M., et. al, 2012).

By differentiating hiPSCs into neurons, scientists have discovered new data about BD. For example, 12-week bipolar neurons differentiated from hiPSCs when pretreated with Lithium, a drug commonly used to treat BD, showed decreased calcium transients and wave amplitudes similar to controls (Chen, H. M., et. al, 2014). Comparing BD versus control neurons, another study suggests that gene expression in bipolar neurons and neural progenitor cells (NPCs) derived from hiPSCs is altered in candidate genes involved in psychiatric disorders in comparison to controls. One gene called CACNA1C (O'Shea, K. S., & McInnis, M. G., 2016).

encodes an L-type, calcium alpha 1C subunit gene that according to several genome wide association studies (GWASs), has a single nucleotide polymorphism (SNP) at rs1006737 from G to A which is highly associated with BD (Sklar, P., et. al., 2008; Ferreira, M. A., et. al., 2008). Given the high degree of heritability of BD and GWASs performed, CACNA1C is one susceptibility gene that merits further research and is investigated in this study (Uemura, T., Green, M., & Warsh, J. J., 2016).

Although hiPSC-derived neurons provide a better method for modeling development and the genetic underpinnings of BD than animal models or postmortem tissue, one limitation of in vitro neuronal cell culture is that neurons are grown in a 2-dimensional plane. Instead, brain organoids serve as a convincing alternative due to their three-dimensional nature and ability to self-organize, which is more representative of the human brain (See Figure 1).

Whereas 2-D in vitro cell models are usually differentiated using protocols that form only single cell types such as astrocytes, brain organoids can self-organize and give rise to many cell types. Very similar to in vivo embryonic development, hiPSCs can independently form embryoid bodies that consist of 3 germ layers: endoderm, mesoderm, and ectoderm via a gastrulation-like process (McCauley, H. A., & Wells, J. M., 2017). By inhibiting the BMP4 and Nodal pathways with dual SMAD inhibitors for example, ectodermal tissue can be committed to a neural fate, which can give rise to many neural cell types such as astrocytes, neurons, etc. (Chavali, V.R.M., Haider, N., Rathi, S. et al., 2020). Independent organization within brain organoids proceeds much like the human brain via growth factors such as BDNF, creating new ways to alter cellular signaling pathways and derive patterned brain organoid regions (Farhadi, H. F., et. al., 2000). In the case of BD, brain organoids can provide a feasible model to identify potential genetic underpinnings, especially with susceptibility genes like CACNA1C. This can be done by creating isogenic iPSC

lines in which CRISPR-Cas9 gene editing is used to correct a suspected gene variant such as rs1006737 in CACNA1C and determining if this rescues the mutant phenotype (Amin, N. D., & Paşca, S. P., 2018).

Derived ultimately from hiPSCs induced to form neuroectoderm, brain organoids were first used to model microcephaly, demonstrating that this in vitro method is capable of recapitulating human brain development and potentially other neuropsychiatric diseases as well (Lancaster, M. A., 2013). In the complex case of BD, brain organoids offer a model with enough regional diversity to allow investigations to be conducted on multiple cell types at once. Brain organoid culture, unlike neurons grown in 2-D, allows cells to be grown in suspension, thereby providing a more convincing model of the in vivo human brain. By creating this three dimensional and more mature cellular environment, accurate depictions of BD changes throughout regional development can be identified and used to then test therapeutic drugs specific to BD (Quadrato, G., Brown, J., & Arlotta, P. 2016). The human forebrain forms from an inner stem cell population that migrates to the pial surface. By examining gene/protein expression in the formed layers, it is possible to determine the cell composition of that region. Here we identify morphological differences and transcriptional alterations between hiPSC derived bipolar brain organoids, CRISPR corrected lines, and controls.

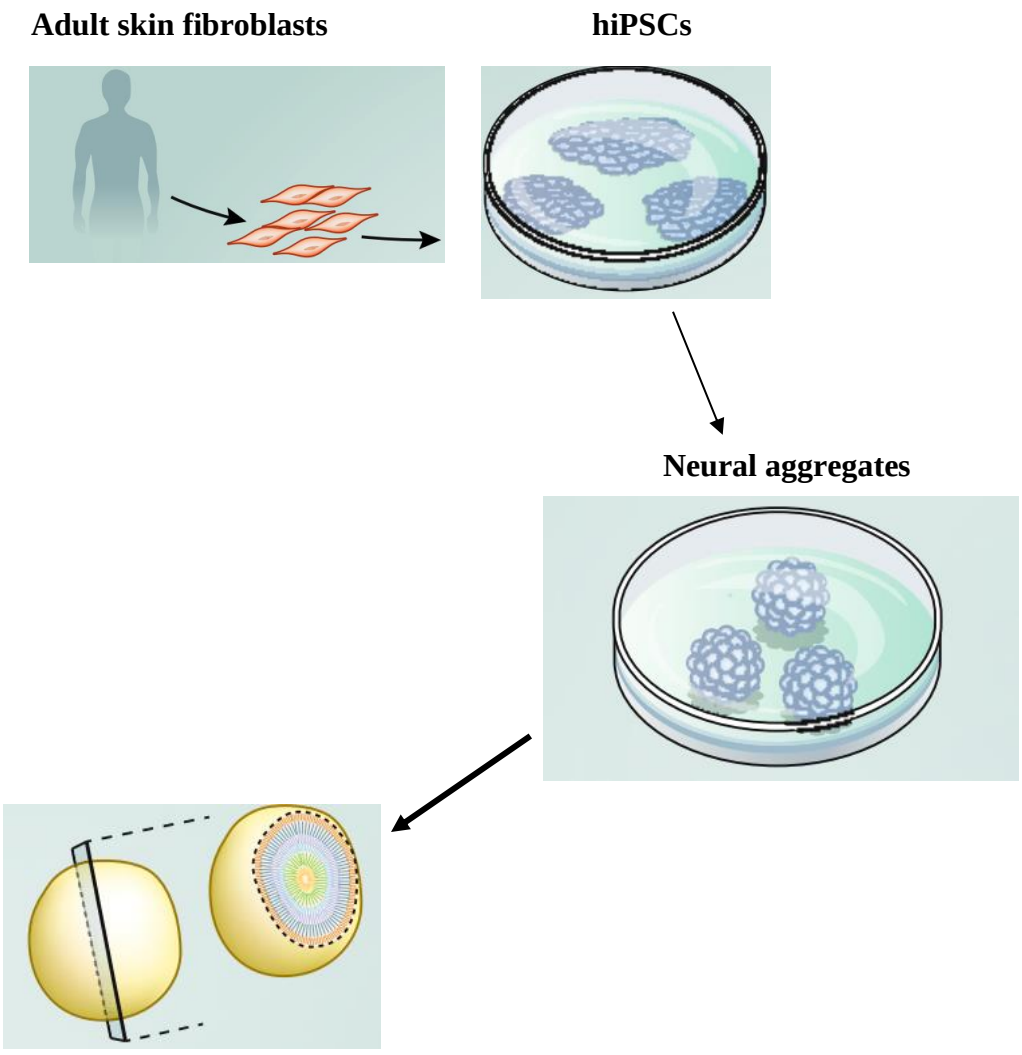

Figure 1: Generation of brain organoids from adult fibroblasts (Pasca, S., 2018).

Methods:

Culture and generation of cerebral organoids from hiPSCs

Skin biopsies were obtained from bipolar patients carrying the "AA" variant in the CACNA1C gene from "GG" control patients, expanded in vitro, and were subsequently reprogrammed to form hiPSC lines. 4 control (C5G, C8WW, C10V, C9G), 4 bipolar (BP17A, BP18A, BP19D, BP11E), and 3 CRISPR (BP17A CRISPR, BP18A CRISPR, BP19D CRISPR) corrected hiPSC cell lines were grown on 60mm TC dishes (Corning, Cat. No. 354004) coated with 0.083mg/mL of Matrigel (Corning, Cat. No. 356234) in DMEM (Gibco, Cat. No. 11054020). hiPSCs were maintained in E8 medium (Stem Cell Technologies, Cat. No. 05991). Upon reaching 80% confluence, hiPSCs were washed once with Dulbecco's phosphate buffered saline without calcium or magnesium (DPBS -/-) (Gibco, Cat. No. 14190136) and passaged using L7 (Lonza, Cat. No. 5013). To generate embryonic bodies, 80% confluent hiPSCs were washed with DBPS -/- and treated with Accutase (Millipore, Cat. No. SCR005) dissociation reagent for 90 seconds at 37°C. After 90 seconds, Accutase was removed, hiPSCs were triturated to make a single cell suspension using E8 media. hiPSCs were collected in a 15mL conical tube and centrifuged at 1000 rpm for 3 min at room temperature. The pellets of the hiPSCs were resuspended in E8 media supplemented with Y27632 (ROCK inhibitor, Tocris, Cat. No. 1254) to inhibit cell death and were plated in a 96-well U bottom plate (Costar, Cat. No 07-200-95) at 20,000 cells per well to form embryoid bodies.

After 48 hours, embryoid bodies were carefully transferred to 6 well ultra-low attachment plates (Costar, Cat. No. 3471) and media was changed to hiPSC media with 2ml per well for the next 4 days. hiPSC media consists of DMEM/F12 with HEPES (Gibco, Cat. No. 11330032),

KOSR (Gibco, Cat. No. 10828-028), MEM NEAA (Gibco, Cat. No. 11140-050), GlutaMAX (Gibco, Cat. No. 35050-061), 2-Mercaptoethanol [0.1mM] (Sigma-Aldrich, Cat. No. M3148), and FGF-2 [10ng/mL] (Peprotech, Cat. No. 100-18B-250UG).

From day 6-25 hiPSC media was changed to neural induction medium (NIM) with 3ml per well to induce neuroectoderm formation. NIM media consists of DMEM/F12, KOSR, MEM NEAA, GlutaMAX, Penstrep (Gibco, Cat. No. 15140122), 2-Mercaptoethanol, Dorsomorphin inhibitor [5µM] (Cayman Chemical, Cat. No. 11967), and SB inhibitor [10µM] (Cayman Chemical, Cat. No. 13031). Dorsomorphin inhibitor and SB inhibitor are used to inhibit BMP and nodal signaling to promote forebrain neuroectoderm differentiation.

Neuroectoderm typically forms after 5 days and after that neural spheroids become patterned forebrain organoids in a 6 well ULA plate with 4ml of NDM (neural differentiation medium). NDM consists of Neurobasal medium (Gibco, Cat. No. 21103-049), B27 (Gibco, Cat. No. 17504-044), GlutaMAX, Penstrep, EGF [20ng/mL] (Peprotech, Cat. No. AF100-15), FGF-2 [20ng/mL], NT3 [20ng/mL] (Peprotech, Cat. No. 450-03-10UG), GDNF [20ng/mL] (Peprotech, Cat. No. 450-10-50UG) and BDNF [20ng/mL] (Peprotech, Cat. No. 450-02-50UG). Brain organoids were maintained with NDM media for long-term growth. Protocol was modified from Sloan, S.A., et. al, 2018.

Organoid Imaging and Analysis:

On day 6, neural spheroids were imaged at 5x on a Leica DMi1 inverted microscope. Images were uploaded to ImageJ where each file was scaled, thresholded, and analyzed to obtain spheroid area in mm^2. Any fused spheroids or those cut off from the images were not analyzed.

ImageJ “smooth” technique was used to mitigate debris from appearing in the threshold and being counted as an organoid. Average spheroid circularity was recorded for each cell line and subsequently an unpaired two-tailed t-test was performed using Graphpad Prism to identify any significant differences between pairs of control, bipolar, and CRISPR corrected spheroid cell lines.

RNA Isolation, PCR, and Quantitative PCR:

Day 30, 60, and 90 brain organoid samples for each cell line were collected and washed once with DPBS -/-. RNA was isolated using Qiagen RNeasy mini kit and RNase-Free DNase set (Qiagen, Cat. No. 74104). RNA concentrations were measured using a Nanodrop machine (Thermo Scientific, Cat. No. 2000-C) and stored at -80°C until further use. Complimentary DNA was prepared by reverse transcription using the SuperScript III First-Strand Synthesis SuperMix for RT-qPCR (Thermo Fisher, Cat. No. 18080051). qPCR was conducted in a 96 well plate (Applied Biosystems, Cat. No. 4346906) using Applied Biosystems QuantStudio 3 (Cat. No. A28571) where all samples were run in triplicates. Target and housekeeping genes used in this study (*PAX6, GFAP, GAD67, VGLUT-1, CACNA1C, and GAPDH*) are presented in table 1:

Table 1: Primers for target genes for qPCR

Gene	Description	Forward Primer	Reverse Primer	Cat. No. Forward/Reverse
CACNA1C	L-type, calcium alpha 1C subunit gene	TGGTCAATGAGAATACGAGG	CCATAGTTGGAACCTTGGTG	F: 128228336 R: 128228337
GAD67	GABA synthesis marker	TCAAGTAAAGATGGTGATGGGATA	GCCATGATGCTGTACATGTTG	F: 135869932 R: 135869933
PAX6 Harvard-1	Neural progenitor cell marker	TGGGCAGGTATTACGAGACTG	ACTCCCGCTTATACTGGGCTA	F: 89456445 R: 89456446
VGLUT-1	Glutamatergic marker	GAAGCTGCACCGCCTTCT	CAGACCACTCATGATGGCGA	F: 119444635 R: 119444636
GFAP	Astrocyte marker	CTGCTCAATGTCAAGCTG	AATGGTGATCCGGTTCTC	F: 187782686 R:187782687
GAPDH	Housekeeping gene	TCATTTCCTGGTATGACAACGA	GGTCTTACTCCTTGGAGGC	F:141545794 R:141545795

All qPCR samples were ran for 40 cycles of 95°C at 3 minutes and 30 seconds, 60°C for 30 seconds, 72°C for 35 seconds followed by a melt curve of 95°C for 15 seconds, 60°C for 1 minute, and 95°C for 15 seconds. Gene expression analysis was normalized to the *GAPDH* housekeeping gene and expressed as fold change compared to controls day 30, 60, and 90. To analyze for significance, an unpaired Welch corrected two-tailed t-test was performed on samples grouped by day and by cell line.

Cryosectioning:

Organoids were washed in Dulbecco's phosphate buffered saline with calcium and magnesium (DPBS +/+) to preserve the cytoskeleton (Thermofisher, Cat. No. 14040141), fixed with 4% PFA (Electron Microscopy Sciences, Cat. No. 15700) for 10 minutes and stored at 4°C in DPBS+/+. Fixed samples were flash frozen in O.C.T. embedding compound (Fisher Scientific, Cat. No. 4585) in tissue pathology disposable base molds (Thermo Scientific, Cat. No. 41-741). 10 and 20 µm tissue sections were cut using a microtome (Thermo Scientific, Cat. No. HM525NX), collected onto microscope slides (Fisherbrand, Cat. No. 12-550-15), and stored at -80°C.

Immunohistochemistry:

Tissue sections were brought to room temperature and washed with DPBS +/+ to remove excess O.C.T.. Sections were permeabilized with 0.1% Triton (Sigma-Aldrich, Cat. No. T9284-500ML) and 0.1% Sodium Citrate (CalBioChem, Cat. No. 567446) in DPBS +/+. Samples were then washed twice with DPBS +/+ and blocked with 10% Normal Donkey Serum (Jackson ImmunoResearch, Cat. No. 017-000-121) containing 10% Triton and 10% Sodium Azide (Sigma-Aldrich, Cat. No. S2002-5G) in DPBS +/+. After blocking, samples were stained for the following proteins with primary antibodies and stored overnight at 4°C in table 2:

Table 2: Primary Antibodies used for Immunohistochemistry

Primary Antibody	Description	Dilution	Company/Cat. No.
Tubb3-Ck	Tubulin present in neuron axons	1:500	Abcam, Cat. No. AB107216
Pax6- Ms	Neural progenitor cell marker	1:500	Millipore, Cat. No. MAB5552
Nkx2.1-Rb	Transcription factor involved with early neuron migration	1:250	Abcam, Cat. No. AB76013
Vglut-1-Gp	Glutamatergic marker	1:500	Millipore, Cat. No. AB5905
Neun-Ms	Neuronal nuclei marker	1:100	Millipore, Cat. No. MAB377
Gad67-Rb	GABA marker	1:500	Abcam, Cat. No. AB49832
PV-Ms	Specialized GABA marker	1:500	Millipore, Cat. No. MAB1572
GFAP-Gt	Astrocyte marker	1:100	Santa Cruz, Cat. No. SC-6170
Syn1-Rb	Synapse marker	1:200	Cell Signaling, Cat. No. 5297

The following day tissue samples were washed twice with DPBS +/+ and stained in the dark for 30 minutes with secondary antibodies in table 3:

Table 3: Secondary Antibodies used for Immunostaining

Secondary Antibody	Dilution	Company/Cat. No.
Green 488 Dk anti Ck (Tubb3)	1:500	Jackson Immunoresearch, Cat. No. 703545155
Orange 555 Dk anti Ms (Pax6)	1:500	Alexa Fluor, Cat. No. A31570
Red 594 Dk anti Rb (Nkx2.1)	1:500	Jackson Immunoresearch, Cat. No. 711585152
Green 488 Dk anti Gp (Vglut-1)	1:500	Jackson Immunoresearch, Cat. No. 706545148
Orange 555 Dk anti Ms (Neun)	1:500	Alexa Fluor, Cat. No. A31570
Red 594 Dk anti Rb (Gad67)	1:500	Jackson Immunoresearch, Cat. No. 711585152
Orange 555 Dk anti Ms (PV)	1:500	Alexa Fluor, Cat. No. A31570
Green 488 Dk anti Gt (GFAP)	1:500	Santa Cruz, Cat. No. sc-2020
Purple 647 Dk anti Rb (Syn1)	1:500	Jackson Immunoresearch, Cat. No. 711605152

Samples were once again washed with DPBS +/+ and stained with a 1:1000 dilution of Hoechst (Thermo Fisher, Cat. No. 33258) for 5 minutes to stain DNA. Samples were then washed with DPBS +/+ and 1mm thick coverslips (Electron Microscopy Sciences, Cat. No. 71887-03) were applied with Prolong Gold antifade mounting media (Thermo Fisher, Cat. No. P36930). Slides were left to dry and stored at room temperature in the dark. Samples were examined using DAPI, GFP, Cy3, and Cy5 filters and were imaged on a Leica DMi8 fluorescent microscope at 5x and 10x. Single channel images were merged with 497.5um and 248.7um for the scale bars respectively.

Results:

Discrepancies in circularity among control, bipolar, and CRISPR corrected lines suggest differences in cell division and differentiation:

To determine if control, BP, and CRISPR cell lines grew similarly in the same culture conditions (see Methods), cerebral spheroids were imaged on day 6 prior to neural induction (Figure 2). To analyze morphological differences, circularity was measured for n = 100 spheroids per cell line and results were graphed and analyzed for significance with a two-tailed unpaired t-test (Figure 3). BP cell lines showed a significant decrease in circularity compared to control and CRISPR lines ($p \leq 0.0001$ and $p \leq 0.001$ respectively) which appear to be more radially organized. Circularity between controls and CRISPR lines however exhibited no significant differences in circularity. These results suggest that BP cell lines may have undergone less organized cellular division and differentiation than control and CRISPR lines by day 6. Also, differences in circularity between control and CRISPR groups were not significant, consistent with our expectations that control groups should have similar circularity compared to CRISPR groups. Therefore, other measurements of proliferation and differentiation may be useful such as circumference or diameter.

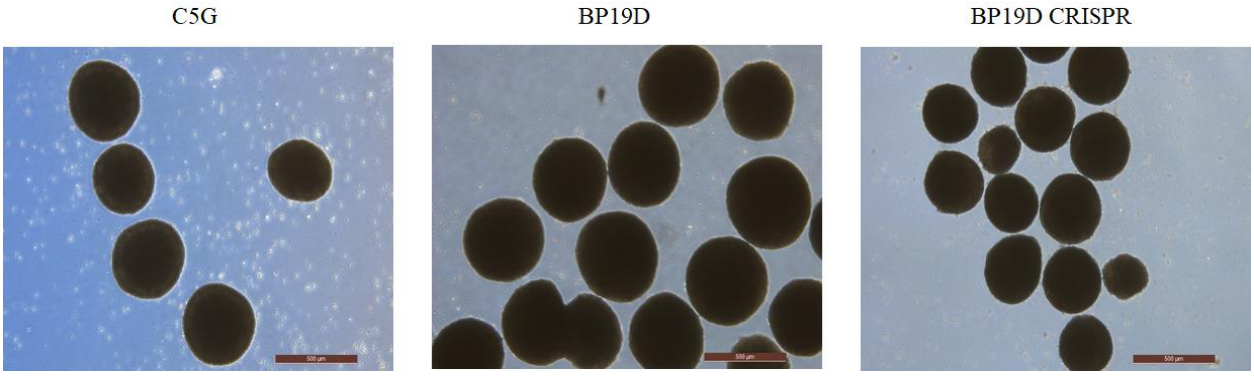

Figure 2: 5x images of day 6 cerebral spheroids in control (C5G), bipolar (BP19D), and CRISPR corrected (BP19D CRISPR) cell lines illustrating morphological differences between various groups. Scale bar 500um

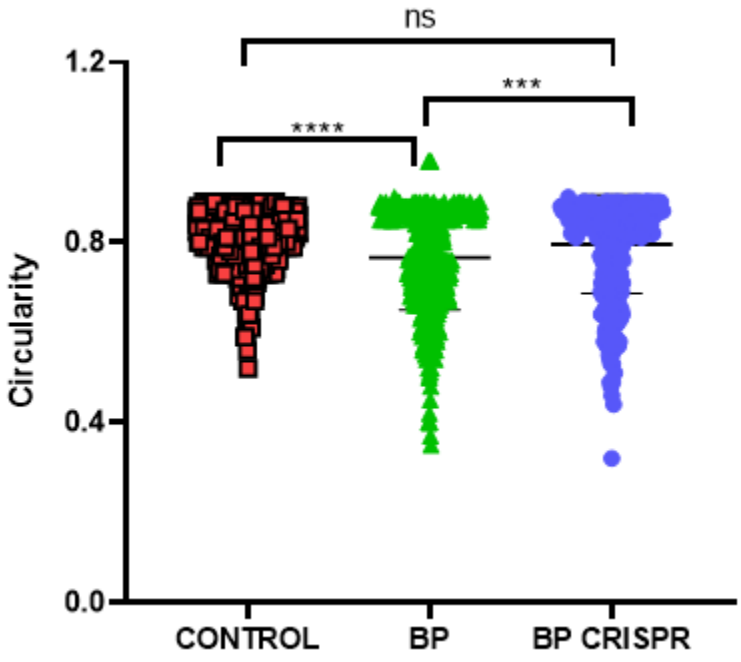

Figure 3: Distribution and statistical analysis of a measure of circularity between various groups. Circularity is a proxy for cell division and differentiation. *** = $p \leq 0.001$, **** = $p \leq 0.0001$

Comparison of fold change in neural gene expression shows increasing levels of PAX6, VGLUT-1, and GAD67 at various stages of brain organoid development:

To investigate transcriptional alterations throughout early brain organoid development among control, BP, and CRISPR lines, qPCR was performed with C5G, BP19D, and BP19D CRISPR on day 30, 60, and 90 samples for 5 transcripts (see Table 1). Using *GAPDH* as a housekeeping gene, a global control day 30 normalized fold change curve was generated for *PAX6*, *GFAP*, *VGLUT-1*, *GAD67*, and *CACNA1C* (Figure 4). Overall, these preliminary results show significant increased fold change levels for *PAX6*, *VGLUT-1*, and *GAD67* throughout development.

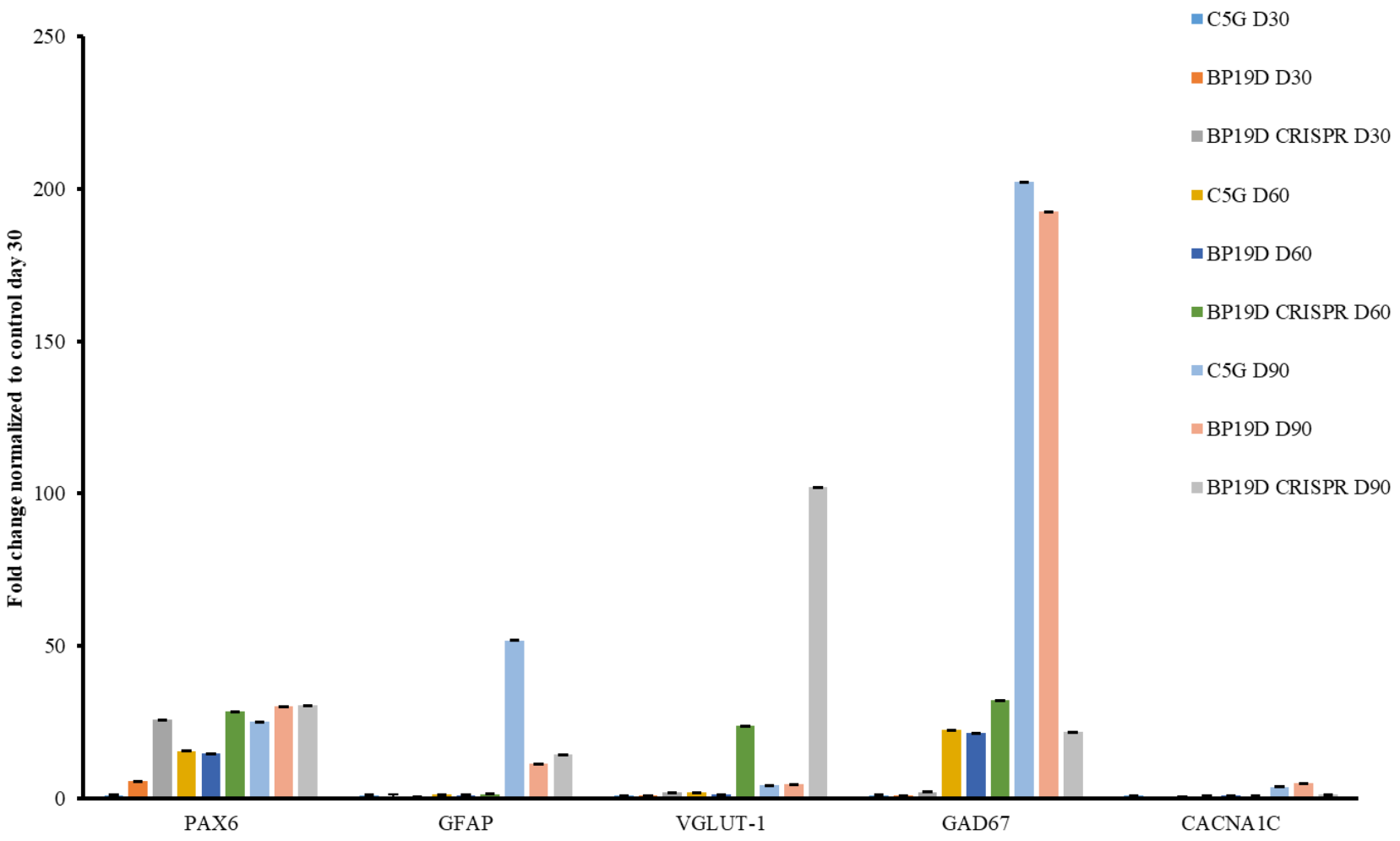

Figure 4: Global comparison of fold change in neuronal gene expression in lines C5G, BP19D, and BP19D CRISPR on days 30, 60, and 90.

Normalized fold changes on day 30 show an approximate 5-fold and 26-fold increase in expression of the early neural marker *PAX6* in BP19D and BP19D CRISPR respectively relative to C5G (Figure 5A). Fold change increases in *GFAP*, *VGLUT-1*, *GAD67*, and *CACNA1C* were similar across BP and CRISPR corrected groups as well. These two observations are consistent with each other since *PAX6* is a neural progenitor cell (NPC) marker and low expression of neuron markers such as *VGLUT-1* (glutamatergic neuron marker) and *GAD67* (GABA neuron marker) showed that these neurons have not yet matured in day 30 samples.

Examining normalized fold changes on day 60, expression of *PAX6* decreases and *VGLUT-1* fold change levels become significantly higher (relative to BP19D for C5G and BP19D CRISPR) (Figure 5B). *GAD67* fold change levels also rise compared to day 30 but are expressed at varying levels across all three cell lines at day 60. These results suggest an increase in the presence of glutamatergic neurons at day 60 in BP19D CRISPR relative to C5G. This is maybe due to the differentiation of NPCs that were previously enriched at day 30. For fold changes normalized and grouped by day 90, BP19D CRISPR still showed higher *VGLUT-1* expression relative to C5G. In addition, fold change levels of all other markers do not show much change in relation to C5G at day 90 (Figure 5C).

When analyzing fold changes in target genes on days 30, 60, and 90 normalized to day 30 samples of each cell line, *PAX6*, *VGLUT-1*, and *GFAP* all consistently increased as brain organoids matured from day 30 to day 90 (Figures 6-8). *GAD67* fold change levels are significantly higher in C5G and BP19D than *VGLUT-1* suggesting a higher presence of GABA neurons than glutamatergic (Figure 6B/D and 7B/D). It is worth noting that *GAD67* levels decreased from day 60 to day 90 in BP19D CRISPR cell lines possibly because as neurons expressing GABA mature, they start to down regulate the synthesis of *GAD67* (Figure 8D).

GFAP is an astrocyte marker that usually does not appear until day 120, yet it showed in day 90, indicating early differentiation of astrocytes (Figure 6C, 7C, 8C). *GFAP* levels at day 90 were considerably lower in BP19D and BP19D CRISPR compared to C5G. Also, changes in *CACNA1C* levels appear to be highest during day 90 for each line however the highest fold change occurred in BP19D on day 90 for reasons unknown (Figure 6E, 7E, 8E).

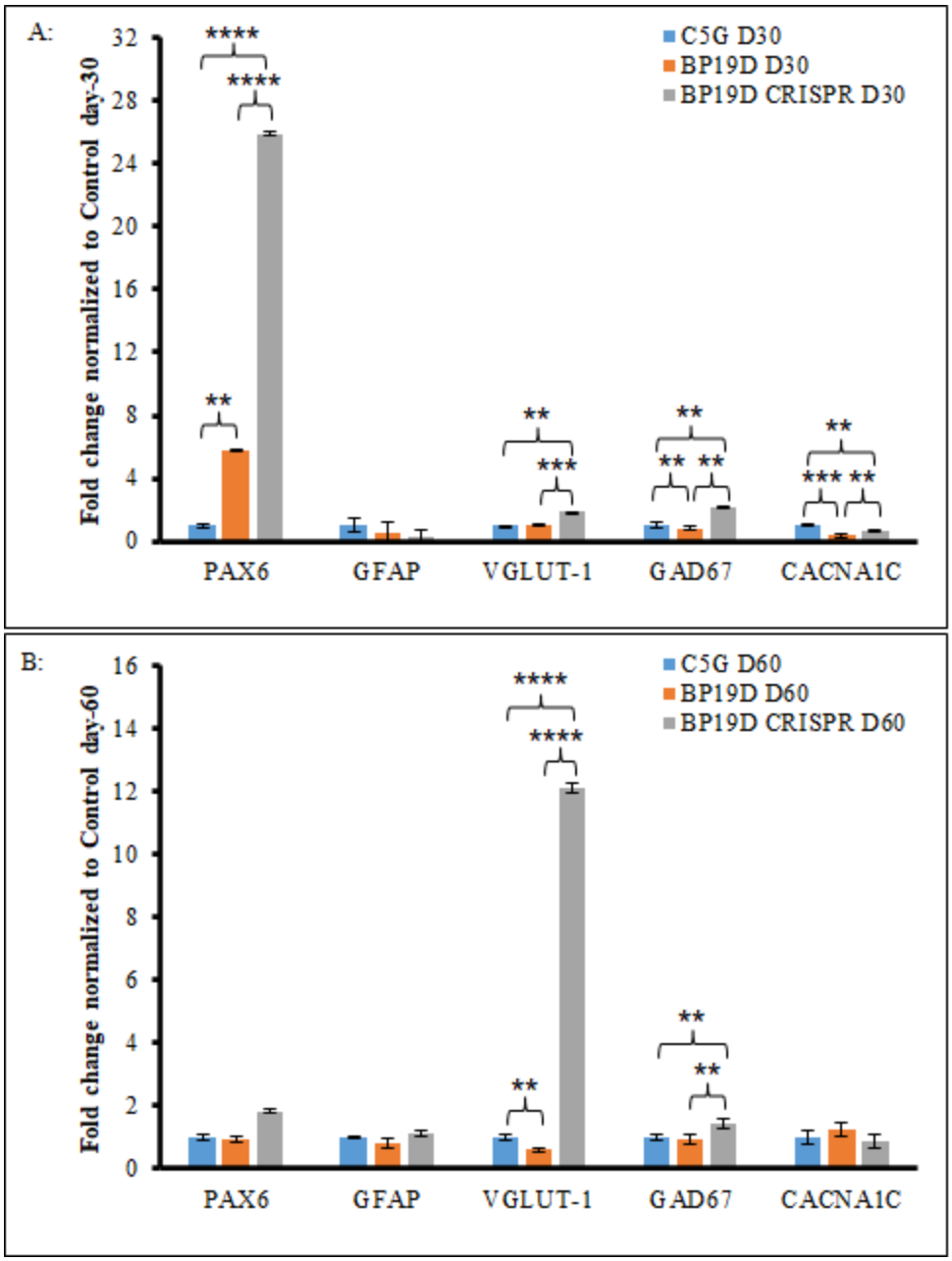
A:
Fold change normalized to Control day-30
32
28
24
20
16
12
8
4
0
C5G D30
BP19D D30
BP19D CRISPR D30
****
****
**
**
***
**
**
**
***
**
PAX6
GFAP
VGLUT-1
GAD67
CACNA1C
B:
Fold change normalized to Control day-60
16
14
12
10
8
6
4
2
0
C5G D60
BP19D D60
BP19D CRISPR D60
****
****
**
**
**
PAX6
GFAP
VGLUT-1
GAD67
CACNA1C

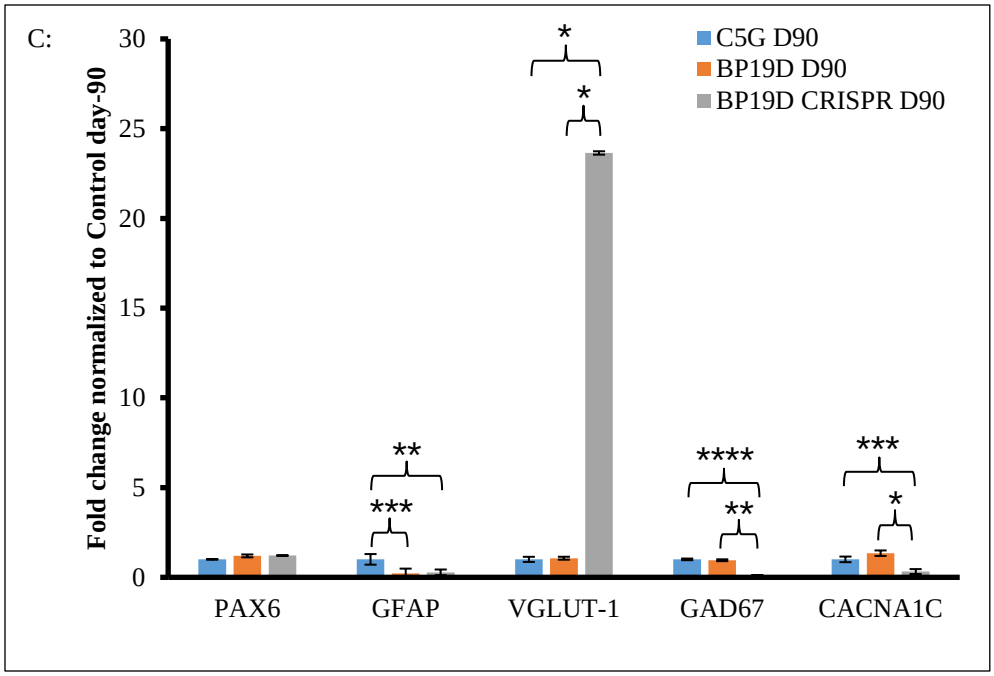

Figure 5: Mean fold change in neural gene expression in lines C5G, BP19D, and BP19D CRISPR on days 30 (A), 60 (B), and 90 (C). * = p≤ 0.05, ** =p≤0.01, *** = p≤0.001, **** = p≤0.0001

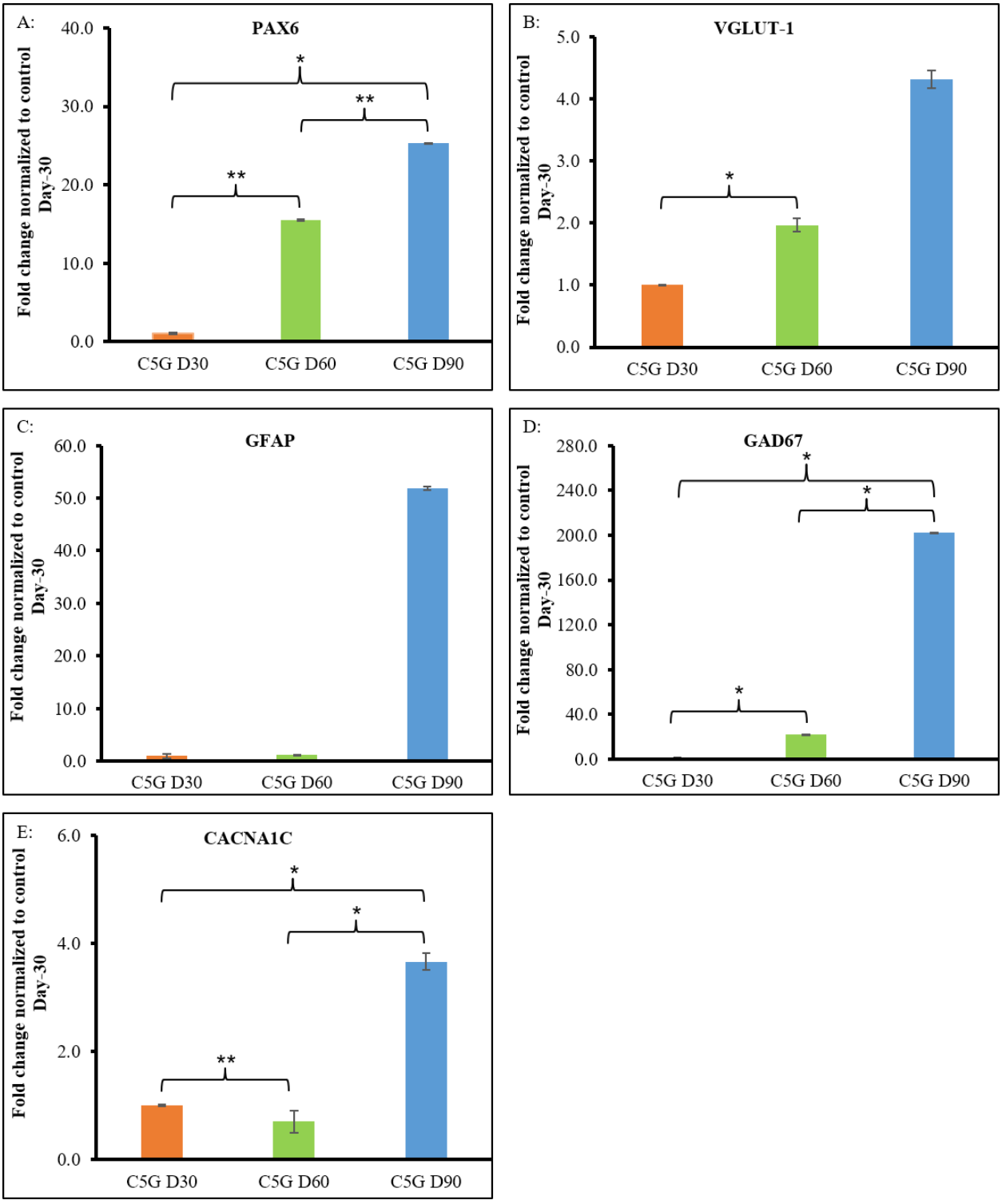

Figure 6: Mean fold change in neural gene expression on day 30, 60, 90 in the C5G line. * = $p \leq 0.05$, ** = $p \leq 0.01$

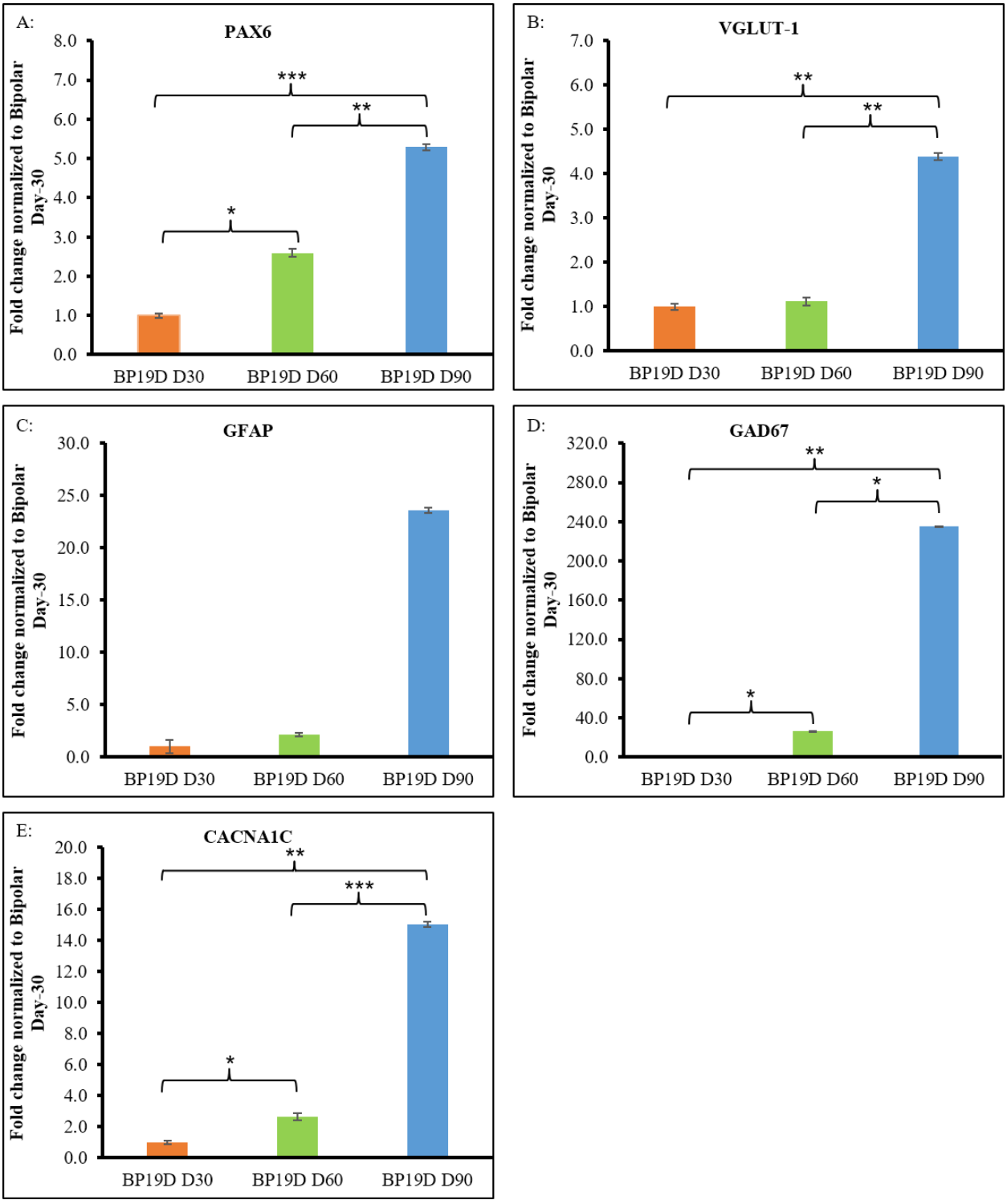

Figure 7: Mean fold change in neural gene expression on day 30, 60, 90 in the BP19D line. * = $p \leq 0.05$, ** = $p \leq 0.01$, *** = $p \leq 0.001$, **** = $p \leq 0.0001$

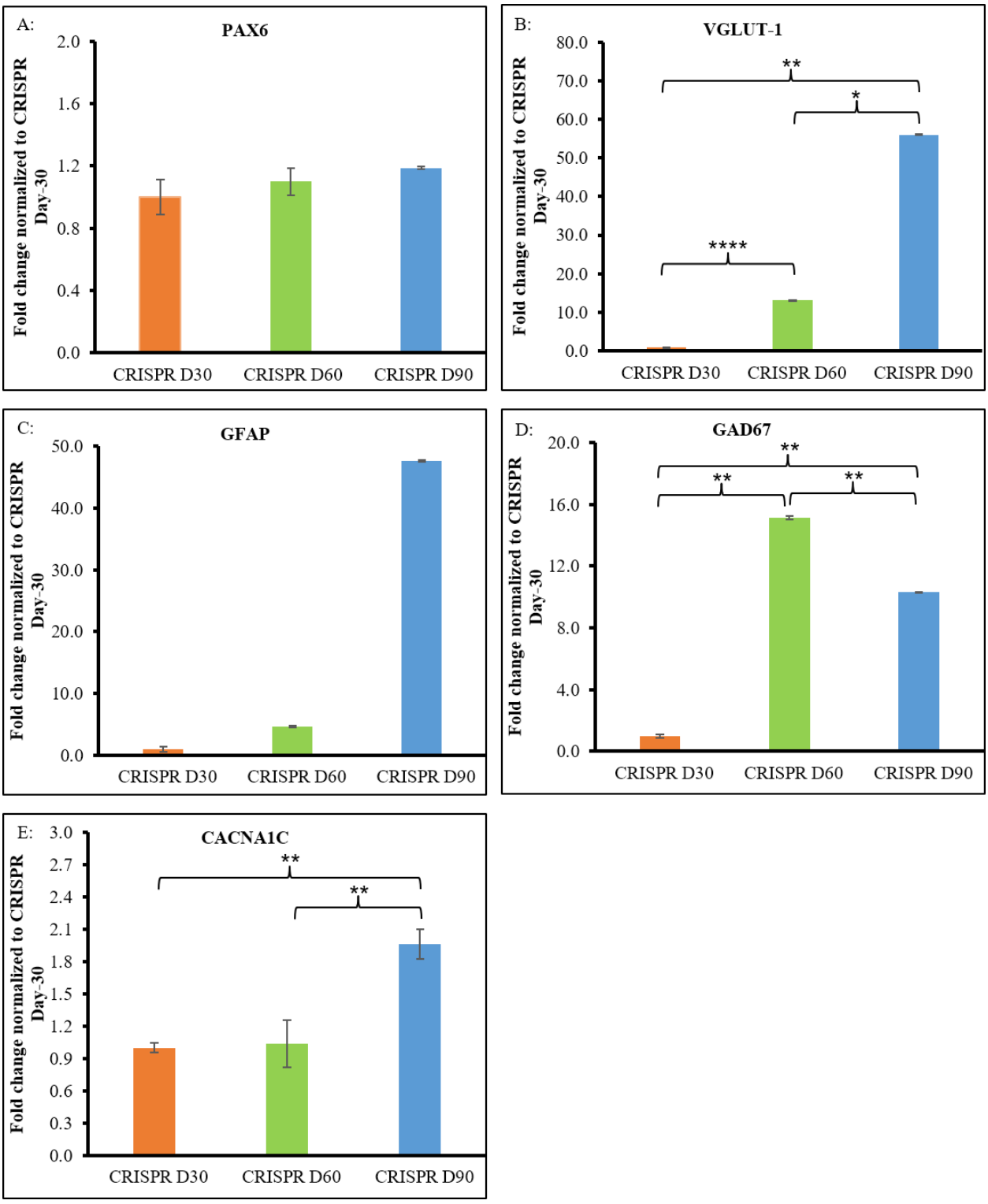

Figure 8: Mean fold change in neural gene expression on day 30, 60, 90 in the BP19D CRISPR line. * = $p \leq 0.05$, ** = $p \leq 0.01$, *** = $p \leq 0.001$, **** = $p \leq 0.0001$

Immunohistochemical localization of neural markers are consistent with qPCR results. Markers not examined by qPCR merit further research:

To evaluate protein expression levels within the brain organoid samples, tissue sections were cut and stained for 9 markers (see Table 2) via immunohistochemistry (IHC). For all day 30 samples, Tubb3 was clearly expressed (Figure 9A and 10A). Tubb3 is a microtubule marker present in neurons. Pax6 was also expressed in all day 30 samples which is concordant with qPCR results (Figure 9A and 10A). In addition, Vglut-1, Gad67, Neun (neuronal nuclei marker), and Nkx2.1 (neuronal migration TF marker) were not detectable except in BP19D CRISPR day 30 samples (Figure 9B and 10B). Furthermore, Syn-1 (neuron synapse marker) was present and Parvalbumin (PV) was absent in all day 30 samples (Figure 9C and 10C). This is expected because PV (specialized GABA neuron marker) usually is expressed later in development (Sloan, S.A., et. al., 2018). GFAP, although usually expressed by day 120, is present in C5G and BP19D CRISPR on day 30 although this is likely due to early differentiation (Figure 9A/C and 10A/C) (Sloan, S.A., et. al., 2018).

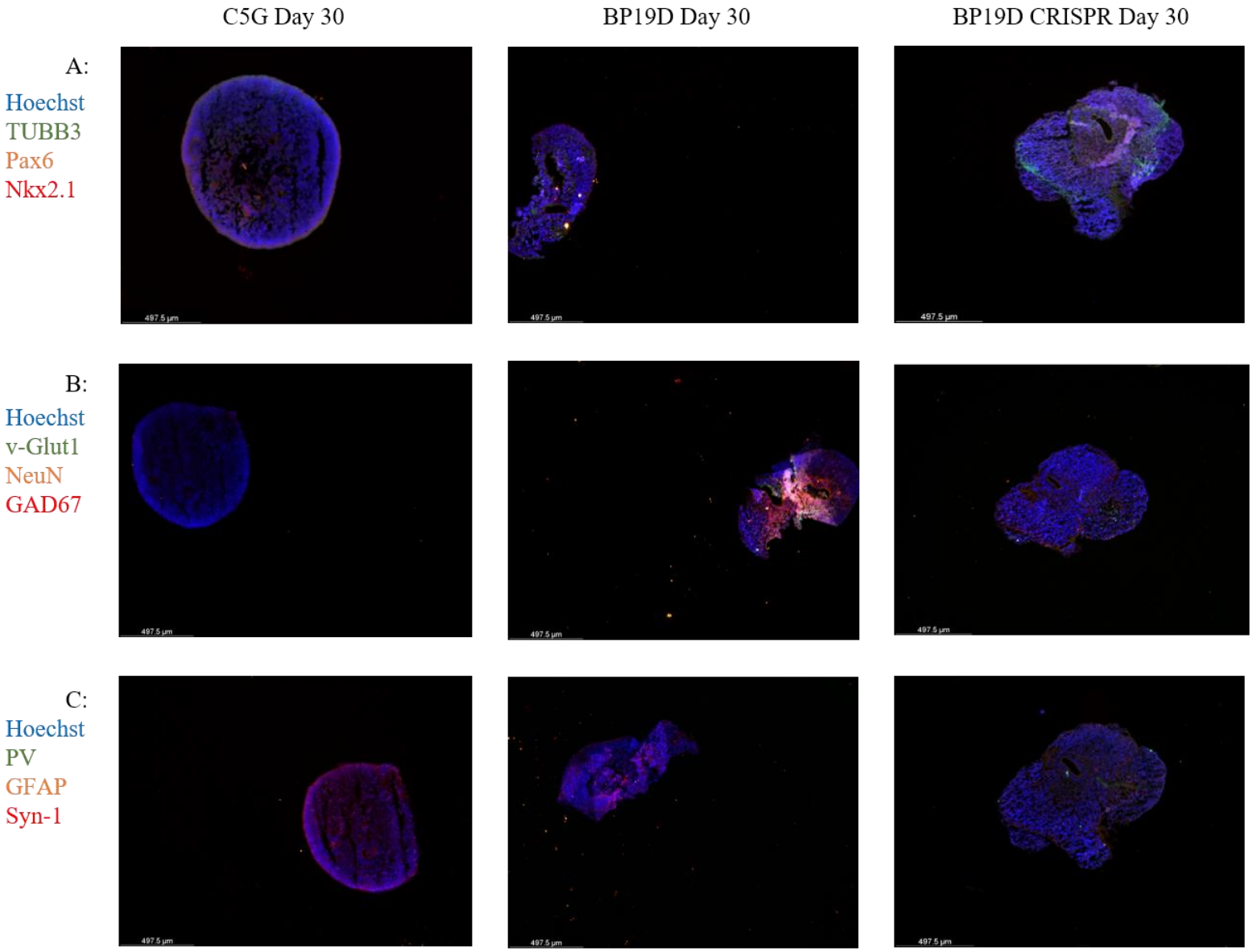

Figure 9: Immunofluorescent (5x) images of day 30 tissue sections. Scale bar 497.5 µm

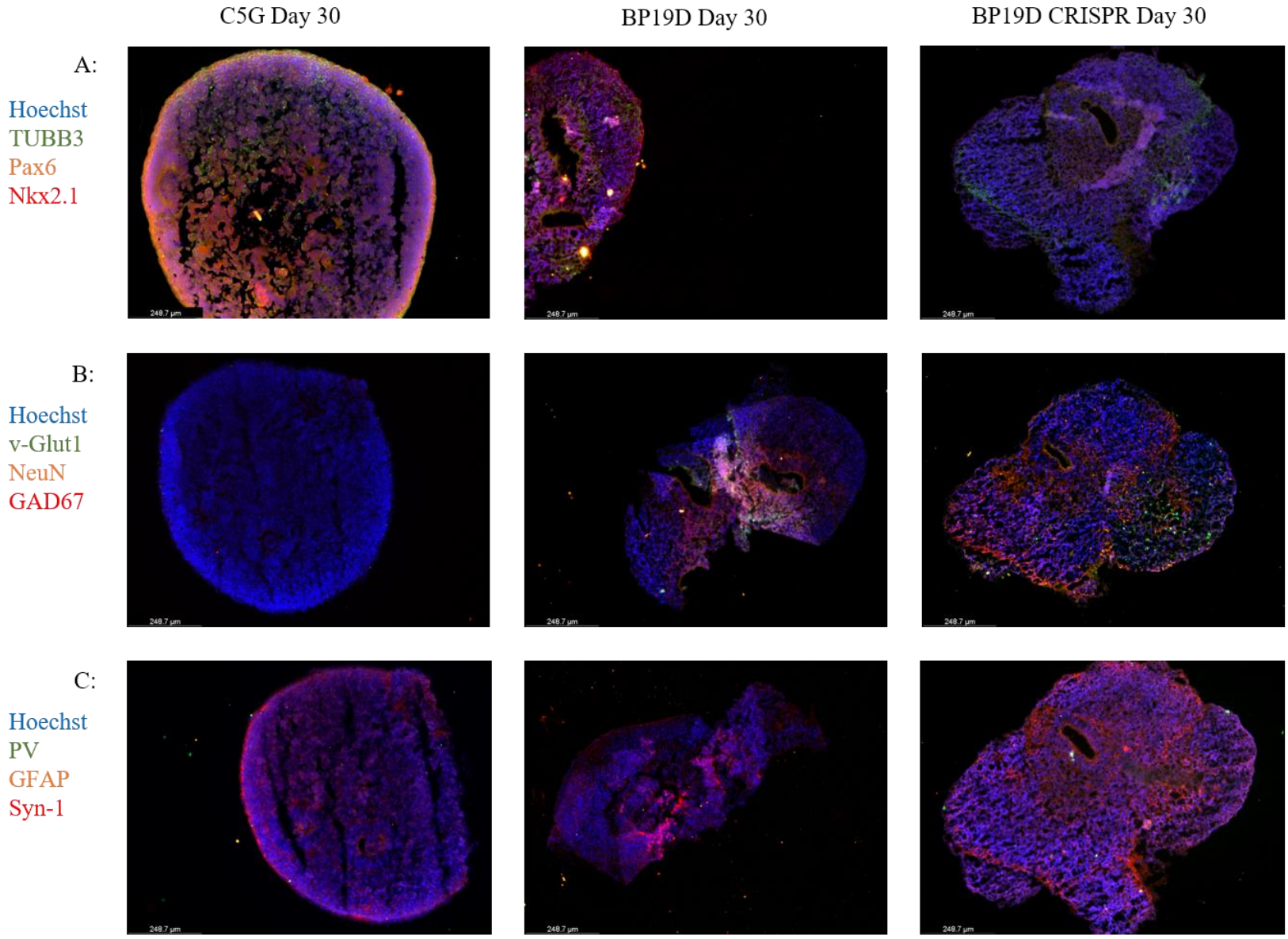

Figure 10: Immunofluorescent (10x) images of day 30 tissue sections. Scale bar 248.7 µm

Day 60 tissue samples were also stained for the same markers and as expected, Tubb3 was present in all day 60 samples (Figure 11A and 12A). In addition, neuronal markers such as Nkx2.1, Vglut-1, Neun, and Gad67 started to become visible too, validating the qPCR results done for *VGLUT-1* and *GAD67* (Figure 11B and 12B). Syn-1 was present in all day 60 samples and PV was not. GFAP was detected in BP19D Day 60 only which also suggests early differentiation within this group (Figure 11C and 12C).

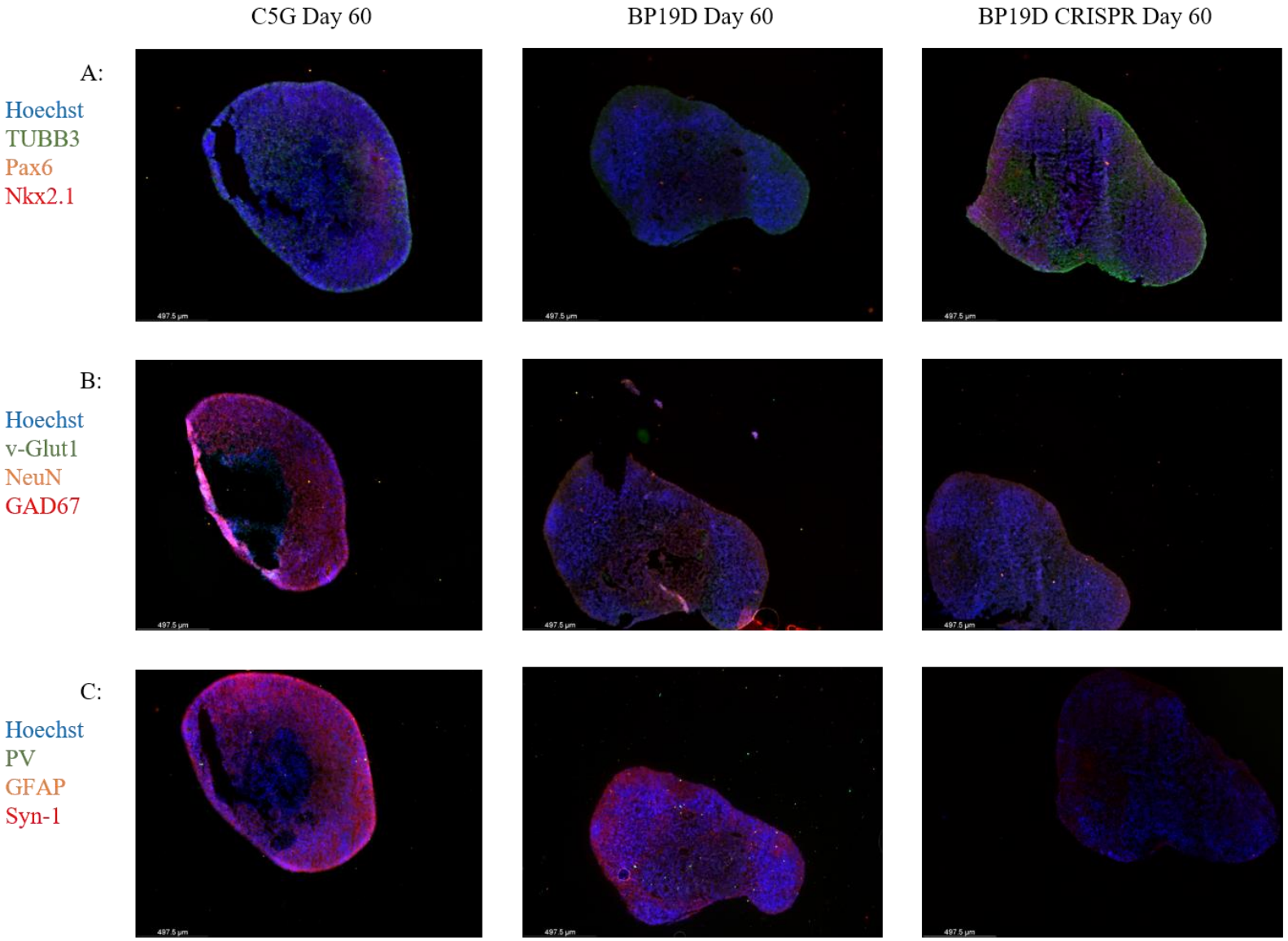

Figure 11: Immunofluorescent (5x) images of day 60 tissue sections. Scale bar 497.5 µm

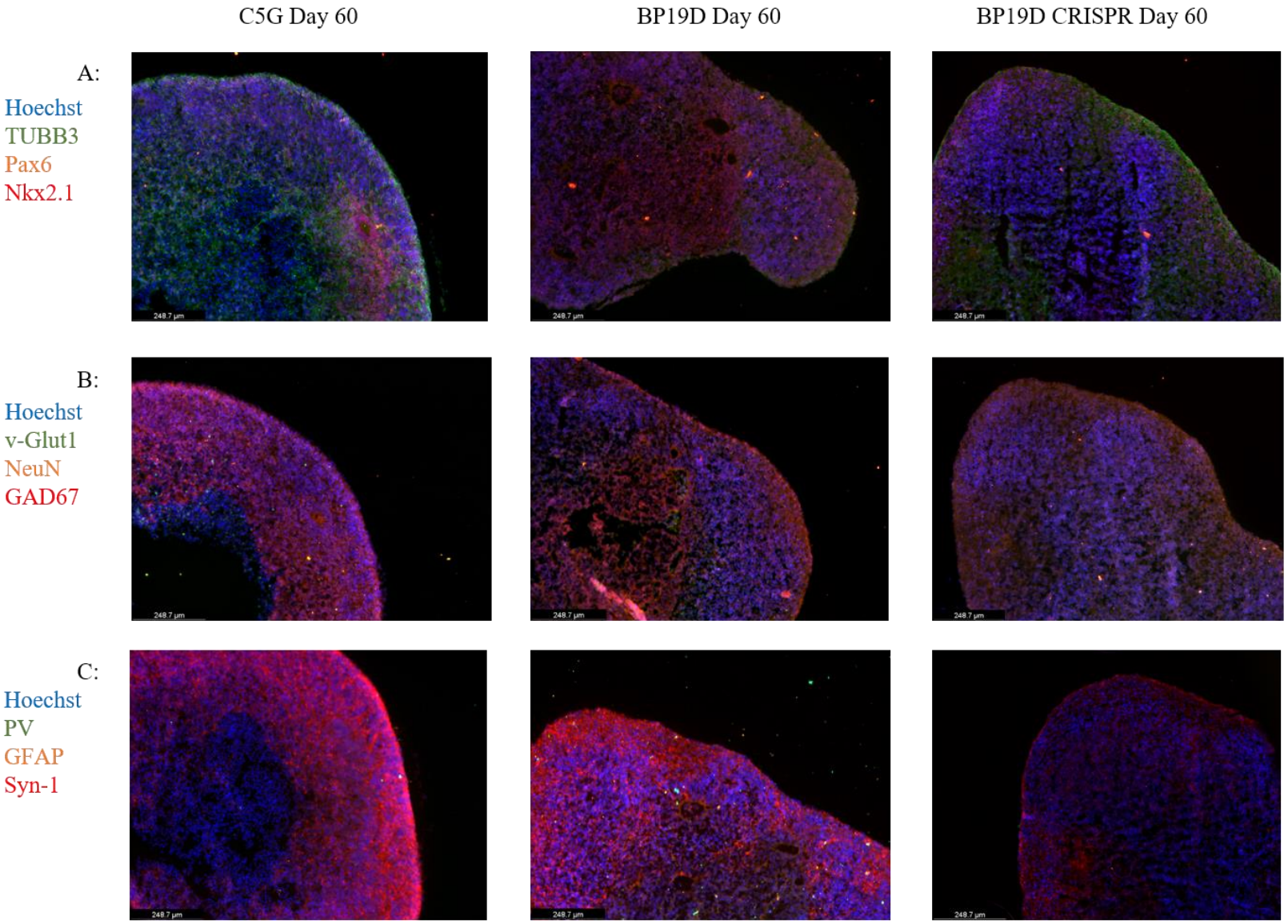

Figure 12: Immunofluorescent (10x) images of day 60 tissue sections. Scale bar 248.7 µm

Tubb3 was detected in all day 90 samples along with Syn-1 (Figure 13C and 14C). GFAP was also present at day 90 in C5G and BP19D CRISPR, suggesting early differentiation in these cell lines. Nkx2.1 was present in C5G and is faintly expressed elsewhere in BP19D and BP19D CRISPR (Figure 13A and 14A). Gad67 was found in C5G and BP19D CRISPR while Neun and Vglut-1 was expressed in BP19D only (Figure 13B and 14B).

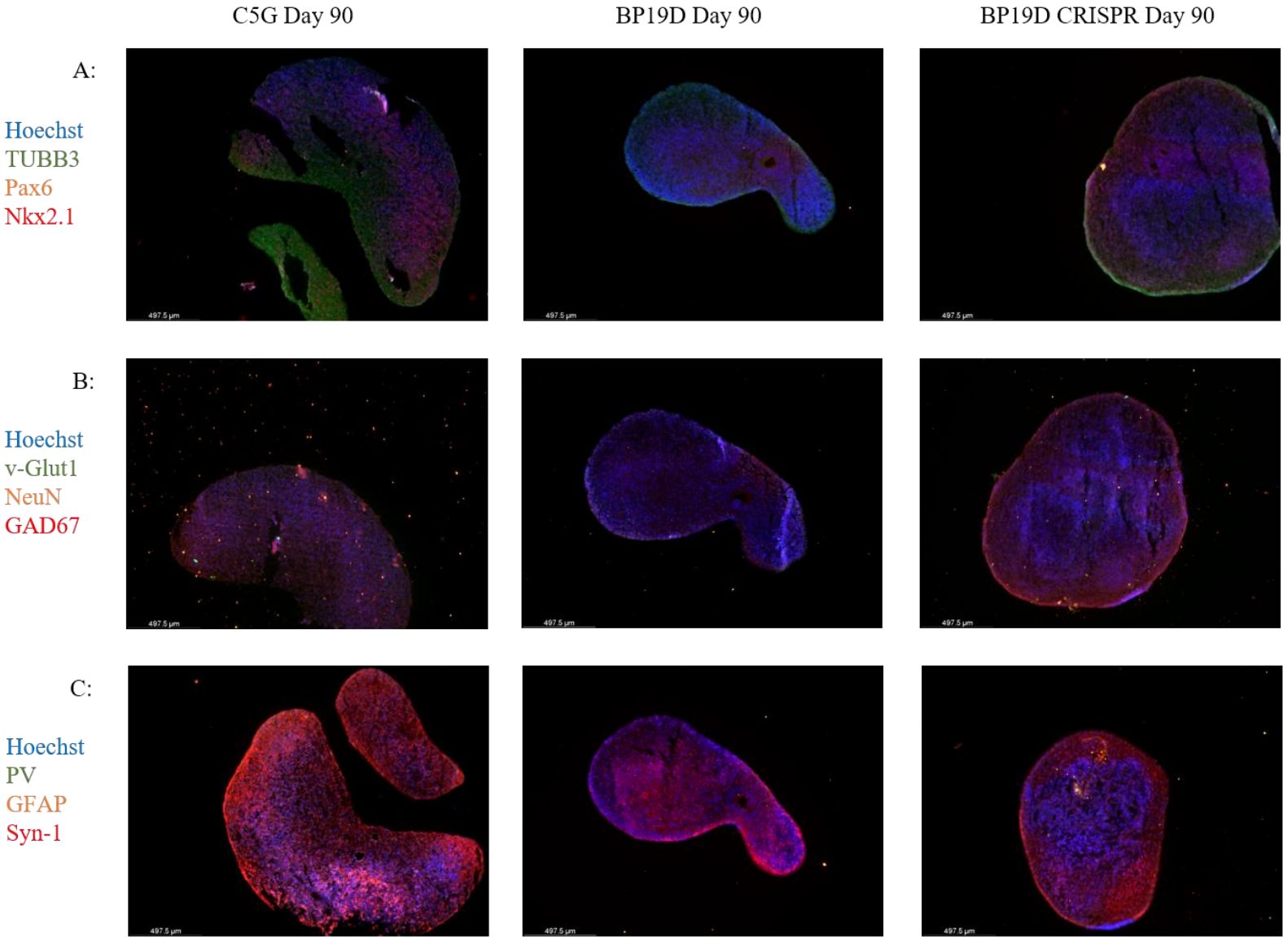

Figure 13: Immunofluorescent (5x) images of day 90 tissue sections. Scale bar 497.5 µm

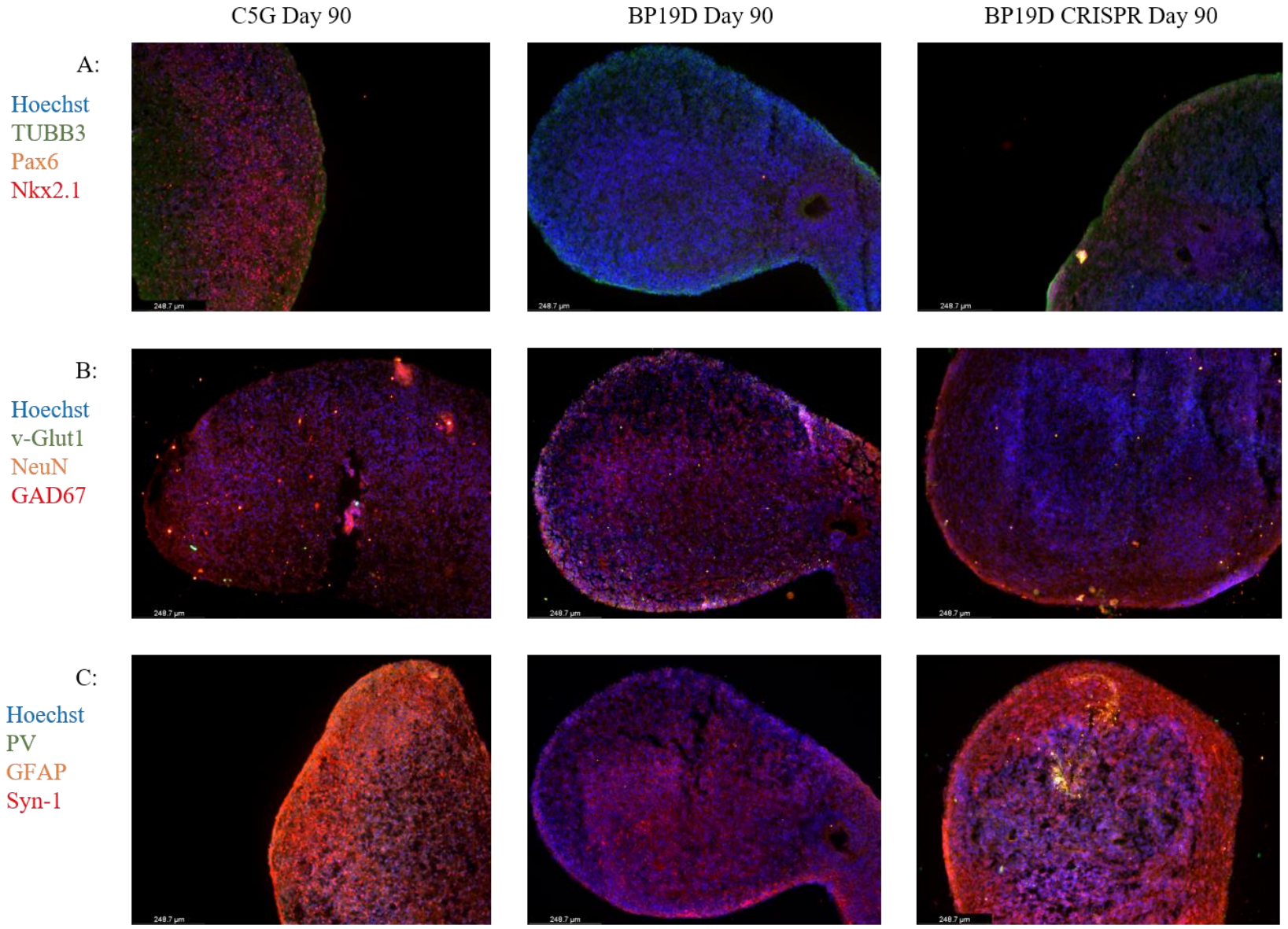

Figure 14: Immunofluorescent (10x) images of day 90 tissue sections. Scale bar 248.7 µm

Discussion:

From qPCR and IHC data, my results suggest that throughout days 30-90 of development, brain organoids gradually give rise to mature neurons and astrocytes. As *PAX6* expression increased, *VGLUT-1* and *GAD67* fold changes gradually increased, illustrating the differentiation of NPCs into mature neurons. This is especially true for BP19D CRISPR which expressed high levels of *PAX6* leading to increased maturation of glutamatergic neurons relative to C5G and BP19D. In addition, *GFAP* was also expressed at the highest level on day 90 for C5G, BP19D, and BP19D CRISPR. Although this astrocyte marker has been reported to be present in day 120 samples, *GFAP* was present at day 90, suggesting that early differentiation of these cells occurred. Furthermore, CACNA1C fold change levels were highest in BP19D on day 90, consistent with CACNA1C levels being higher in BP patients than in control and CRISPR corrected cell lines.

Overall, brain organoids are useful models for studying later stages of forebrain development. Although gene expression assays such as qPCR can be performed in 2D neuronal cultures, 3D organoids allow for identification of later forming glia such as astrocytes. In this capacity, human brain development can be best modeled in brain organoids given their ability to self-organize and give rise to multiple neural lineages. There are also limitations in protein localization for 2D neurons in vitro as well. As evident through immunostaining, brain organoids at later stages of development express different proteins compared to early stages. For example, Vglut-1 and Gad67 were present in day 60 samples, unlike day 30 and GFAP was present in day 90 samples unlike day 30. Also, throughout the developmental stages, protein markers can be detected in different regions of tissue such as the periphery which is where many of these

proteins are expressed. This is because different neural cell types are formed in unique cortical layers of organoid tissue. In vivo, NPCs are found in regions such as the ventricular zone (VZ) and subventricular zone (SVZ) (Figure 15). As brain organoids mature further, deep/upper neuronal markers such as TBR1, SATB2, and CTIP2 start to be detected, forming the cortical plate (CP). Eventually, astrocytes develop and support neuron cell types in the CP. The organization of these cell types in developing brain organoids are similar to that of the fetal human brain, making it feasible to use organoids to model the cellular composition of brains from patients with BD.

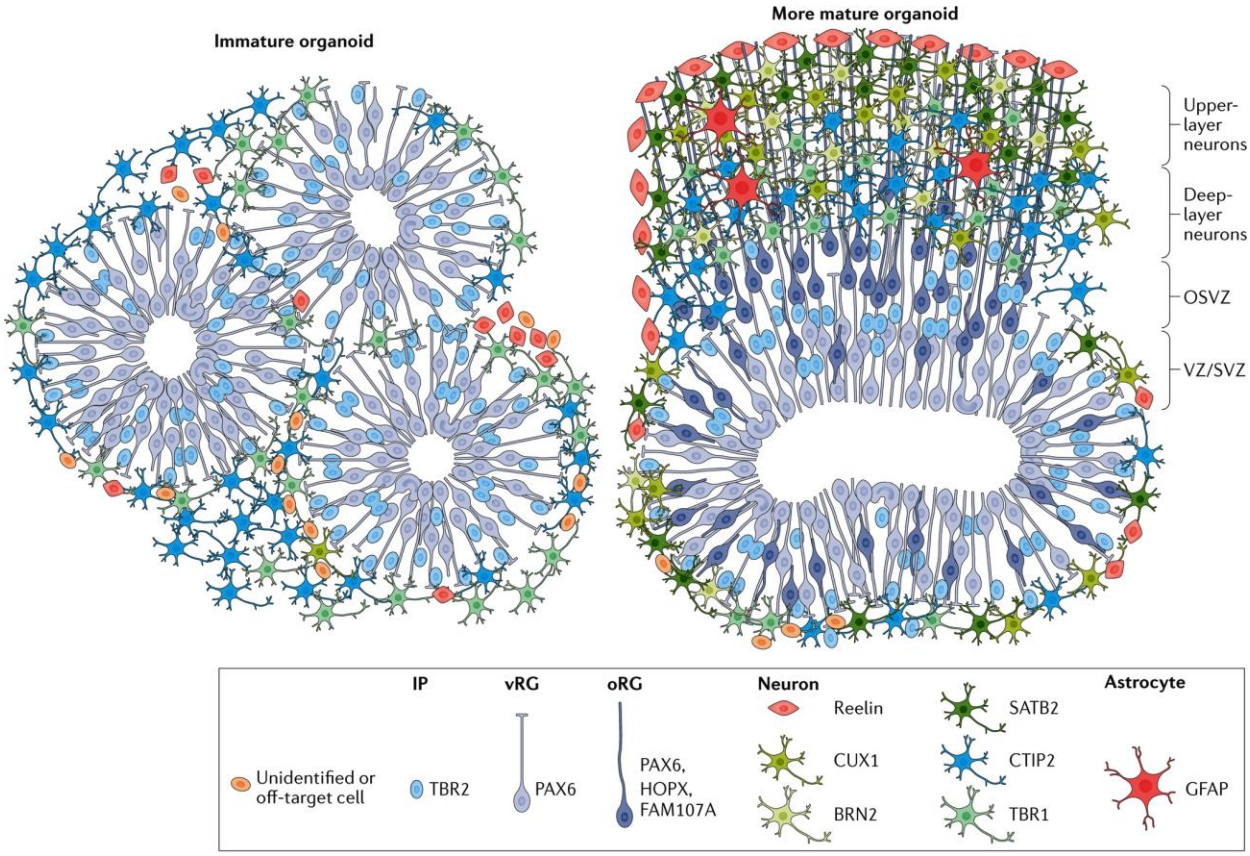

Figure 15: Schematic representation of brain organoid cortical layer development in vitro (Di Lullo, E., & Kriegstein, A. R., 2017).

In addition, the use of CRISPR corrected organoids allows us to better investigate the role of *CACNA1C* (SNP rs1006737) in individuals with BD. Since control and BP cell lines contain the "GG" and "AA" *CACNA1C* variant respectively, by utilizing BP CRISPR cell lines to correct the "AA" variant back to "GG", we can potentially determine if BP CRISPR corrected lines are different compared to BP cell lines. More specifically, BP CRISPR corrected cell lines can elucidate whether the correction of the *CACNA1C* SNP results in transcriptional alterations or protein expression changes in comparison to BP cell lines. This is because we expect BP CRISPR lines to be similar to controls, which was true when we analyzed spherical organization with circularity.

Despite having shown significant differences in gene/protein expression in control, BP, and BP CRISPR corrected brain organoids with development, there is much to be done in order to investigate the underlying cellular mechanisms underlying behaviors of patients with BD. Since only one control, BP, and BP CRISPR corrected line was used so far, additional lines (3 control, 3 BP, and 3 BP CRISPR corrected) are being analyzed for a larger sample to examine for variations in gene or protein expression.

Additionally, more genes should be examined to identify the patterns underlying BD. Although a few genes were examined in qPCR, more genes need to be measured. For these reasons, transcriptome analysis via bulk RNA sequencing of control, BP, and CRISPR corrected cell lines is currently being carried in 3 lines each, to screen for approximately 22,000 genes in the sequencing core. From there, any additional genes of interest will be validated with qPCR and IHC.

Furthermore, while IHC data has allowed us to validate qPCR results of additional genes such as Syn-1, Nkx2.1 and PV should be examined. However, this work only provides a

snapshot of protein expression in one organoid section. Instead, additional IHC of serial sections should be performed to better understand specifically where certain protein markers localize. By staining multiple slices of a particular organoid, 3D computer generated models can be developed to characterize protein localization overall. Furthermore, since brain organoid sections were cut at 10µm and 20µm, perhaps higher resolution imaging techniques such as confocal microscopy should be used to effectively image organoids that have different depths.

Long term organoid culture is needed to understand gene and protein expression levels past day 90. As previously mentioned, CACNA1C and GAD67 level fold changes normalized to BP19D day 30 were highest in the BP19D day 90 sample along with GFAP in all day 90 samples. By examining brain organoids at even later stages of development such as day 200 or 8 months, perhaps additional changes in gene and protein expression could be observed for example, the appearance of other cell markers such as the specialized GABA gene Parvalbumin. 8-month unpatterned organoids samples have been harvested and collected but not yet analyzed.

Also, in addition to patterning forebrain organoids, fused assembloids may merit further research. Having already cultured dorsal forebrain organoids, fusing ventral forebrain spheroids with dorsal may provide more insight into BD. By fusing the dorsal and ventral forebrain spheroids together, GABAergic neurons from the ventral forebrain can migrate to the dorsal side and integrate to network with cortical glutamatergic neurons (Sloan, S.A., et. al., 2018). By generating these assembloids, neural circuit formation could potentially be characterized from control, BP, and BP CRISPR corrected cell lines. In addition, electrophysiology experiments such as patch clamp could be performed on region specific cells of assembloids to better ascertain neuron specific interactions in 3D cultures (although this fails to capture global analysis (Passaro, A. P., & Stice, S. L., 2021)). Live calcium imaging can also be used to analyze network

activity although in small specific regions of interest (ROI) only. Therefore, recent advancements in microelectrode arrays and optogenetics may compensate for limitations in patch clamp and calcium imaging in brain organoids, since spatial and temporal resolutions are maintained. While more and more advances are being made with brain organoids, there is much to learn about BD.

Acknowledgments:

Thesis committee: I would like to thank the thesis committee for taking the time to evaluate my thesis.

Thesis readers: I would like to thank professors Sue O'Shea, Sara Aton, and Haoxing Xu for agreeing to read my thesis despite their busy schedules.

Sponsors/Mentors: I would like to thank Sue O'Shea and Sara Aton for agreeing to co-sponsor my research in the MCDB department. I would also like to thank Durga Attili for being an outstanding mentor who has taken the time to teach me a lot about countless scientific concepts.

Lab members: I would like to thank Cindy DeLong, Durga Attili, and Dan Schill for showing me how to culture stem cells. I would also like to thank Dan Schill and Durga Attili for showing me how to perform qPCR. I would like to thank Durga Attili and Guihua Jiang for showing me how to do IHC, and Kate Campbell for keeping me company on late nights in the lab. Last but not least I would like to thank Sue O'Shea for giving me the opportunity to be in this lab and supporting me every step of the way.

Funding:

Funding: I would like to acknowledge and thank the Prechter, Tam, and Beld funds in addition to the NIH (NIMH U19-106434) for funding this research.

Here's to a better pandemic free year and bright future ahead...

References

Amin, N. D., & Paşca, S. P. (2018). Building Models of Brain Disorders with Three-Dimensional Organoids. Neuron, 100(2), 389–405. https://doi.org/10.1016/j.neuron.2018.10.007

Baldessarini, R. J., Tondo, L., Baethge, C. J., Lepri, B., & Bratti, I. M. (2007). Effects of treatment latency on response to maintenance treatment in manic-depressive disorders. Bipolar disorders, 9(4), 386–393. https://doi.org/10.1111/j.1399-5618.2007.00385.x

Chavali, V.R.M., Haider, N., Rathi, S. et al. (2020). Dual SMAD inhibition and Wnt inhibition enable efficient and reproducible differentiations of induced pluripotent stem cells into retinal ganglion cells. Sci Rep 10, 11828 . https://doi.org/10.1038/s41598-020-68811-8

Chen, H. M., DeLong, C. J., Bame, M., Rajapakse, I., Herron, T. J., McInnis, M. G., & O'Shea, K. S. (2014). Transcripts involved in calcium signaling and telencephalic neuronal fate are altered in induced pluripotent stem cells from bipolar disorder patients. Translational psychiatry, 4(3), e375. https://doi.org/10.1038/tp.2014.12

Christian K.M., Song H., Ming G. (2012). Application of reprogrammed patient cells to investigate the etiology of neurological and psychiatric disorders Frontiers in Biology, 7 (3) , pp. 179-188. https://doi.org/10.1007/s11515-012-1216-0

Di Lullo, E., & Kriegstein, A. R. (2017). The use of brain organoids to investigate neural development and disease. Nature reviews. Neuroscience, 18(10), 573–584. https://doi.org/10.1038/nrn.2017.107

Farhadi, H. F., Mowla, S. J., Petrecca, K., Morris, S. J., Seidah, N. G., & Murphy, R. A. (2000). Neurotrophin-3 sorts to the constitutive secretory pathway of hippocampal neurons and is diverted to the regulated secretory pathway by coexpression with brain-derived neurotrophic factor. The Journal of neuroscience : the official journal of the Society for Neuroscience, 20(11), 4059–4068. https://doi.org/10.1523/JNEUROSCI.20-11-04059.2000

Ferreira, M. A., O'Donovan, M. C., Meng, Y. A., Jones, I. R., Ruderfer, D. M., Jones, L., Fan, J., Kirov, G., Perlis, R. H., Green, E. K., Smoller, J. W., Grozeva, D., Stone, J., Nikolov, I., Chambert, K., Hamshere, M. L., Nimgaonkar, V. L., Moskvina, V., Thase, M. E., Caesar, S., … Wellcome Trust Case Control Consortium (2008). Collaborative genome-wide association analysis supports a role for ANK3 and CACNA1C in bipolar disorder. Nature genetics, 40(9), 1056–1058. https://doi.org/10.1038/ng.209

GBD 2017 Disease and Injury Incidence and Prevalence Collaborators (2018). Global, regional, and national incidence, prevalence, and years lived with disability for 354 diseases and injuries for 195 countries and territories, 1990-2017: a systematic analysis for the Global Burden of Disease Study 2017. Lancet (London, England), 392(10159), 1789–1858. https://doi.org/10.1016/S0140-6736(18)32279-7

Gordovez, F., & McMahon, F. J. (2020). The genetics of bipolar disorder. Molecular psychiatry, 25(3), 544–559. https://doi.org/10.1038/s41380-019-0634-7

Kim, Y., Santos, R., Gage, F. H., & Marchetto, M. C. (2017). Molecular Mechanisms of Bipolar Disorder: Progress Made and Future Challenges. Frontiers in cellular neuroscience, 11, 30. https://doi.org/10.3389/fncel.2017.00030

McCauley, H. A., & Wells, J. M. (2017). Pluripotent stem cell-derived organoids: using principles of developmental biology to grow human tissues in a dish. Development (Cambridge, England), 144(6), 958–962. https://doi.org/10.1242/dev.140731

Mendlewicz, J., Rainer, J. (1977) Adoption study supporting genetic transmission in manic–depressive illness. Nature 268, 327–329. https://doi-org.proxy.lib.umich.edu/10.1038/268327a0

Nakagawa, M., Koyanagi, M., Tanabe, K., Takahashi, K., Ichisaka, T., Aoi, T., Okita, K., Mochiduki, Y., Takizawa, N., & Yamanaka, S. (2008). Generation of induced pluripotent stem cells without Myc from mouse and human fibroblasts. Nature biotechnology, 26(1), 101–106. https://doi.org/10.1038/nbt1374

Nestler, E., Hyman, S. Animal models of neuropsychiatric disorders. Nat Neurosci 13, 1161–1169 (2010). https://doi.org/10.1038/nn.2647

O'Shea, K. S., & McInnis, M. G. (2016). Neurodevelopmental origins of bipolar disorder: iPSC models. Molecular and cellular neurosciences, 73, 63–83. https://doi.org/10.1016/j.mcn.2015.11.006

Pasca, S., (2018). Building Three-Dimensional Human Brain Organoids, Nature Neuroscience, https://doi.org/10.1038/s41593-018-0107-3

Passaro, A. P., & Stice, S. L. (2021). Electrophysiological Analysis of Brain Organoids: Current Approaches and Advancements. Frontiers in neuroscience, 14, 622137. https://doi.org/10.3389/fnins.2020.622137

Quadrato, G., Brown, J., & Arlotta, P. (2016). The promises and challenges of human brain organoids as models of neuropsychiatric disease. Nature medicine, 22(11), 1220–1228. https://doi.org/10.1038/nm.4214

Sklar, P., Smoller, J. W., Fan, J., Ferreira, M. A., Perlis, R. H., Chambert, K., Nimgaonkar, V. L., McQueen, M. B., Faraone, S. V., Kirby, A., de Bakker, P. I., Ogdie, M. N., Thase, M. E., Sachs, G. S., Todd-Brown, K., Gabriel, S. B., Sougnez, C., Gates, C., Blumenstiel, B., Defelice, M., … Purcell, S. M. (2008). Whole-genome association study of bipolar disorder. Molecular psychiatry, 13(6), 558–569. https://doi.org/10.1038/sj.mp.4002151

Sloan, S. A., Andersen, J., Paşca, A. M., Birey, F., & Paşca, S. P. (2018). Generation and assembly of human brain region-specific three-dimensional cultures. Nature protocols, 13(9), 2062–2085. https://doi.org/10.1038/s41596-018-0032-7

Takahashi, K., Tanabe, K., Ohnuki, M., Narita, M., Ichisaka, T., Tomoda, K., & Yamanaka, S. (2007). Induction of pluripotent stem cells from adult human fibroblasts by defined factors. Cell, 131(5), 861–872. https://doi.org/10.1016/j.cell.2007.11.019

Uemura, T., Green, M., & Warsh, J. J. (2016). CACNA1C SNP rs1006737 associates with bipolar I disorder independent of the Bcl-2 SNP rs956572 variant and its associated effect on intracellular calcium homeostasis. The world journal of biological psychiatry : the official journal of the World Federation of Societies of Biological Psychiatry, 17(7), 525–534. https://doi.org/10.3109/15622975.2015.1019360

Vogt, J., Traynor, R., & Sapkota, G. P. (2011). The specificities of small molecule inhibitors of the TGFß and BMP pathways. Cellular signalling, 23(11), 1831–1842. https://doi.org/10.1016/j.cellsig.2011.06.019

Wen, Z., Christian, K. M., Song, H., & Ming, G. L. (2016). Modeling psychiatric disorders with patient-derived iPSCs. Current opinion in neurobiology, 36, 118–127. https://doi.org/10.1016/j.conb.2015.11.003